Electronic Supplementary Material (ESI) for Dalton Transactions.

- Electronic Supplementary Information -

The Ditungsten Decacarbonyl Dianion

Joseph P. A. Ostrowski,† Benjamin E. Atkinson,† Laurence R. Doyle, Ashley J. Wooles, Nikolas Kaltsoyannis,* and Stephen T. Liddle*

Department of Chemistry, The University of Manchester, Oxford Road, Manchester, M13 9PL, UK.

*E-mail: steve.liddle@manchester.ac.uk; nikolas.kaltsoyannis@manchester.ac.uk

† These authors contributed equally.

Experimental Details

General Considerations

All manipulations were carried out using Schlenk techniques, or an MBraun UniLab glovebox, under an atmosphere of dry nitrogen. Solvents were dried by passage through activated alumina towers and degassed before use. All solvents were stored over potassium mirrors except for ethers which were stored over activated 4 Å sieves. Deuterated solvent was distilled from potassium, degassed by three freeze-pump-thaw cycles and stored under nitrogen. Tungsten hexacarbonyl, potassium, naphthalene, and 18-crown-6 ether were purchased from Sigma Aldrich and dried for 4 hours under vacuum before use.

NMR spectra were acquired on a Bruker AV400 spectrometer operating at 400.2 (^{1}H) and 100.6 (^{13}C{^{1}H}) MHz; chemical shifts are quoted in ppm and are relative to $SiMe_4$. Attenuated total reflectance (ATR) infrared (IR) spectra were obtained using a Bruker Alpha Platinum-ATR FTIR spectrometer or a Thermo Scientific™ Nicolet™ iS™5 FTIR spectrometer with *iD5* ATR accessory. A Horiba XploRA Plus Raman microscope with a 638 nm laser (power: ≤150 mW) was used to obtain all Raman spectra. The power of the laser was adjusted for each sample using a filter to prevent sample decomposition. UV/Vis spectra were obtained using a PerkinElmer Lambda 750 spectrometer. All samples were prepared under a nitrogen atmosphere and collected using a 1 mm path length quartz cuvette. Samples were run *vs.* THF solvent. Electrochemical experiments were carried out using an μAutoLab Type III potentiostat controlled by Nova. Measurements were performed inside a sealed N_2 vessel at room temperature, and subsequently calibrated through the addition of ferrocene. A three-electrode configuration was employed: a Pt working electrode; a Pt wire counter electrode; and an Ag wire pseudo-reference electrode. All electrodes were polished using alumina/H_2O. CHN microanalyses were carried out by Mr M Jennings at the University of Manchester. Crystals were examined using a Rigaku FR-X diffractometer, equipped with a HyPix 6000HE photon counting pixel array detector with mirror-monochromated Mo Kα (λ = 0.71073 Å) or Cu Kα (λ = 1.5418 Å) radiation. Intensities were integrated from a sphere of data recorded on narrow (1.0°) frames by *ω* rotation. Cell parameters were refined from the observed positions of all strong reflections in each data set. Gaussian grid face-indexed absorption corrections with a beam profile correction were applied. The structures were solved either by dual methods using SHELXT[1] and all non-hydrogen atoms were refined by full-matrix least-squares on all unique F^2 values with anisotropic displacement parameters with exceptions noted in the respective cif files. Hydrogen atoms were refined with constrained geometries and riding thermal parameters; U_{iso}(H) was set at 1.2 (1.5 for methyl groups) times U_{eq} of the parent atom. The largest features in final difference syntheses were close to heavy atoms and were of no chemical significance. CrysAlisPro was used for control and integration,[2] and SHELXL and Olex2 were employed for structure refinement.[3,4] ORTEP-3 and POV-Ray were employed for molecular graphics.[5,6]

Preparation of [(OC)$_5$W-W(CO)$_5$][K(18-crown-6)(THF)$_2$]$_2$ (1)

THF (20 ml) was added to a mixture of [W(CO)$_6$] (0.704 g, 2.0 mmol) and 18-crown-6 (0.53 g, 2.0 mmol). THF (20 ml) was then added to a separate mixture of potassium metal (0.08 g, 2.0 mmol) and naphthalene (0.26 g, 2.0 mmol), and the mixture agitated until all the potassium was consumed. The completed potassium naphthalenide solution was added dropwise to the W(CO)$_6$ solution, instantaneously forming a red solution which was allowed to stir over 3 days, resulting in a brown solution. Volatiles were removed *in vacuo* and the resulting brown solid was washed with pentane (2 × 10 ml), then extracted into THF (5 ml) and filtered away from the remaining solid. Volatiles were removed *in vacuo* to afford **1** as a yellow powder. Crystals of **1** suitable for X-ray diffraction were grown from a concentrated THF solution at ambient temperature. Yield: 0.728 g, 58%. Extended drying under vacuum removes the THF as evidenced by the elemental analyses. Anal. Calc'd for $C_{34}H_{48}K_2O_{22}W_2$: C 32.55; H 3.86%. Found: C 32.80; H 3.90%. ^{1}H NMR (500 MHz, d$_8$-THF) δ: 3.64 (48H, s, C*H*$_2$), 3.62 (16H, m, THF(O-C*H*$_2$)), 1.78 (16H, m, THF(CH$_2$-C*H*$_2$)). ^{13}C{^{1}H} NMR (d$_8$-THF) δ: 222.86 (s, W-*C*O) 70.21 (s, O-*C*H$_2$), 66.63 (THF(O-*C*H$_2$)), 23.33 (THF(CH$_2$-*C*H$_2$)). FTIR *v*/cm^{-1} (ATR): 2905 (w), 1938 (m), 1863 (s), 1772 (s), 1467 (w), 1351 (w), 1095 (s), 959 (s), 833 (m), 576 (s). Raman *v*/cm^{-1} (Neat, ≤15 mW): 2019 (w), 1960 (br), 1904 (m), 1794 (w), 595 (w), 447 (s), 405 (m), 97 (vs).

Experimental Data

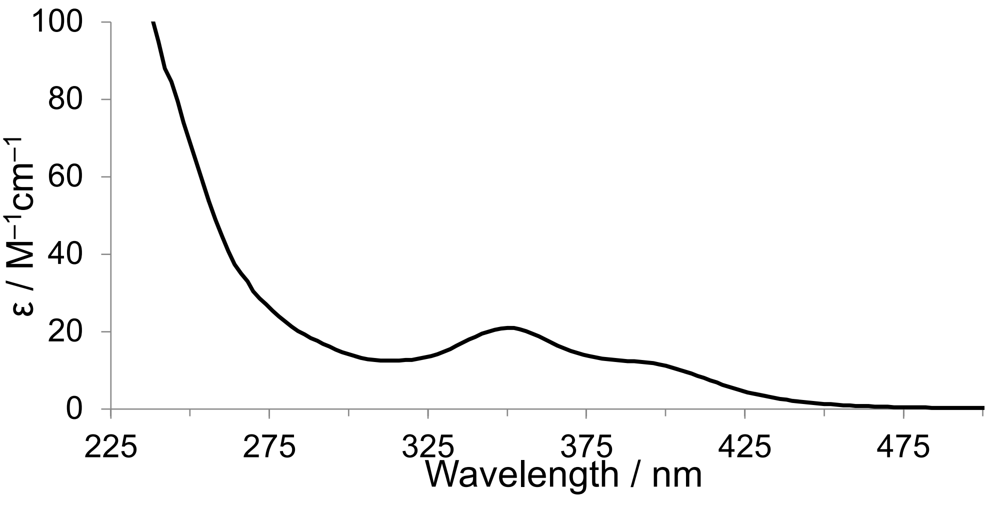

Figure S1. UV/Vis spectrum of complex 1 in THF.

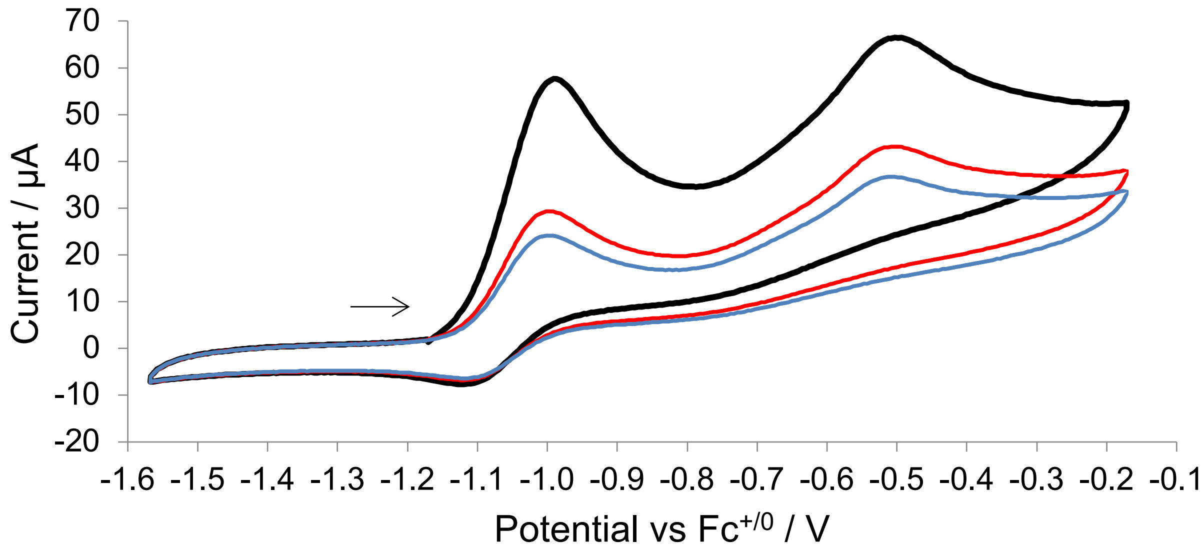

Figure S2. Cyclic voltammogram of 1 (0.42 mM) vs. $Fc^{+/O}$ (2 mM), with [$^{n}Bu_4N$][BF_4] (0.5 M) as electrolyte, showing first (black), second (red) and third (blue) scans. Arrow shows scan directions.

Computational Details

General Considerations

All calculations were performed in Molpro 2018.2.[7] Calculations were performed at the density functional theory (DFT) level of theory, using the hybrid B3LYP[8-11] functional. DFT calculations included dispersion with Grimme's D3 dispersion correction, and Becke-Johnson damping.[12] Additional calculations were performed with spin-coupled scaled second-order Møller–Plesset perturbation theory (SCS-MP2, where singlet excitations are scaled up by 1.2, and triplet excitations down by 1/3, which has previously been shown to perform well for transition metals[13,14]), and coupled cluster with singles, doubles and perturbative triple excitations (CCSD-(T)). Density fitting was employed for DFT and SCS-MP2 calculations.[15] The def2-ATZVPP basis set, from the Molpro basis set library, was used on all elements, alongside the analogous auxiliary basis set for density fitting calculations. This is the def2-TZVPP basis set augmented with one set of diffuse functions,[16,17] and uses the 60 electron quasi-relativistic effective core potential of the

Stuttgart/Cologne Group.[18,19] Calculations were constrained to preserve the four-fold symmetry, *i.e.* D_{4h} when eclipsed, D_{4d} when staggered and D_4 between. Orbital isosurfaces were generated by IBOView.[20] QTAIM calculations were performed with AIMALL version 17.11.14[21] with .wfx files generated by Molden2AIM.[22]

Table S1. Z-matrix used for all calculations

```
W,
W,  1,  BWW,
C,  1,  BCWeq,        2,  ACWWeq,
C,  1,  BCWeq,        2,  ACWWeq,      3,  Deq,   0
C,  1,  BCWeq,        2,  ACWWeq,      4,  Deq,   0
C,  1,  BCWeq,        2,  ACWWeq,      5,  Deq,   0
C,  1,  BCWax,        3,  180.0-ACWWeq, 2,  Dax,   0
O,  1,  BOCeq + BCWeq, 2,  AOWWeq,      6,  Deq,   0
O,  1,  BOCeq + BCWeq, 2,  AOWWeq,      8,  Deq,   0
O,  1,  BOCeq + BCWeq, 2,  AOWWeq,      9,  Deq,   0
O,  1,  BOCeq + BCWeq, 2,  AOWWeq,     10,  Deq,   0
O,  1,  BOCax + BCWax, 3,  180.0-ACWWeq, 2,  Dax,   0
C,  2,  BCWeq,        1,  ACWWeq,      4,  Dspin, 0
C,  2,  BCWeq,        1,  ACWWeq,     13,  Deq,   0
C,  2,  BCWeq,        1,  ACWWeq,     14,  Deq,   0
C,  2,  BCWeq,        1,  ACWWeq,     15,  Deq,   0
C,  2,  BCWax,       13,  180.0-ACWWeq,15,  Dax,   0
O,  2,  BOCeq + BCWeq, 1,  AOWWeq,      4,  Dspin, 0
O,  2,  BOCeq + BCWeq, 1,  AOWWeq,     13,  Deq,   0
O,  2,  BOCeq + BCWeq, 1,  AOWWeq,     14,  Deq,   0
O,  2,  BOCeq + BCWeq, 1,  AOWWeq,     15,  Deq,   0
O,  2,  BOCax + BCWax,13,  180.0-ACWWeq,15,  Dax,   0
[Na, 2,  BOCax + BCWax + 4.0,    13, 180.0 - ACWWeq,   15,  Dax,   0
 Na, 1,  BOCax + BCWax + 4.0,    3,  180.0 - ACWWeq,   2,   Dax,   0]*
```

**B3LYP with explicit Na counter cations only*

The following variables were fixed to preserve four-fold symmetry:

Deq= -90.0°
Dax= 180.0°

Table S2. Energies at the optimized geometries, in Hartree, and energies relative to the staggered (D_{4d}, DSPIN=45°) geometry, in kJ mol^{-1}

	B3LYP		**B3LYP (Na)**		**SCS-MP2**		**CCSD(T)**	
DSPIN:	**E_{el} / Ha**	**ΔE / kJ mol^{-1}**	**E_{el} / Ha**	**ΔE / kJ mol^{-1}**	**E_{el} / Ha**	**ΔE / kJ mol^{-1}**	**E_{el} / Ha**	**ΔE / kJ mol^{-1}**
0	-1267.805545	16.705	-1592.160471	17.247	-1265.085309	18.846	-1265.359032	16.271
5	-1267.805699	16.301	-1592.160632	16.823	-1265.085484	18.387		
10	-1267.806174	15.053	-1592.161129	15.519	-1265.085999	17.035		
15	-1267.806927	13.077	-1592.161882	13.543	-1265.086810	14.906		
20	-1267.807831	10.704	-1592.162838	11.031	-1265.087851	12.174		
25	-1267.808886	7.934	-1592.163925	8.179	-1265.089033	9.069		
30	-1267.809970	5.087	-1592.165053	5.216	-1265.090251	5.872		
35	-1267.810945	2.528	-1592.166123	2.407	-1265.091363	2.952		
40	-1267.811649	0.679	-1592.166805	0.616	-1265.092179	0.809		
45	-1267.811908	0.000	-1592.167040	0.000	-1265.092488	0.000	-1265.365230	0.000

Table S3. SCS-MP2 Optimized variables of the dihedral angle scan, at the SCS-MP2 level of theory[a]

DSPIN	**0[b]**	**5**	**10**	**15**	**20**	**25**	**30**	**35**	**40**	**45***
BWW	3.207714	3.205534	3.198146	3.186576	3.171761	3.155722	3.139449	3.125010	3.114489	3.110459
BCWeq	2.044314	2.044254	2.044253	2.044267	2.044300	2.044198	2.044118	2.044063	2.043978	2.043899
ACWWeq	88.116673	88.064066	87.915310	87.680933	87.358749	86.961957	86.502715	86.025675	85.645275	85.489581
BCWax	1.959445	1.959674	1.960249	1.961236	1.962430	1.963911	1.965453	1.966856	1.967906	1.968386
BOCeq	1.166804	1.166835	1.166917	1.167047	1.167207	1.167384	1.167545	1.167659	1.167725	1.167738
AOWWeq	89.109728	89.041356	88.843500	88.530667	88.097918	87.567329	86.950694	86.307080	85.791849	85.580466
BOCax	1.185489	1.185473	1.185446	1.185401	1.185349	1.185276	1.185209	1.185156	1.185114	1.185096

[a] All bond lengths in Å, angles in ° . [b] used in CCSD(T) single point calculation.

Table S4. B3LYP 2Na Optimized variables of the dihedral angle scan, at the B3LYP level of theory, with explicit Na counter-cations[a]

DSPIN	**0**	**5**	**10**	**15**	**20**	**25**	**30**	**35**	**40**	**45**
BWW	3.314492	3.313175	3.305539	3.294024	3.279057	3.262748	3.246023	3.230976	3.219814	3.216735
BCWeq	2.055137	2.055193	2.055189	2.055158	2.055103	2.055038	2.054971	2.054829	2.054785	2.054755
ACWWeq	87.301779	87.250715	87.121868	86.923234	86.629732	86.299500	85.905615	85.490037	85.196145	85.066023
BCWax	1.929241	1.929309	1.929794	1.930502	1.931502	1.932607	1.933829	1.934963	1.935846	1.936115
BOCeq	1.153515	1.153539	1.153625	1.153754	1.153924	1.154082	1.154227	1.154339	1.154376	1.154386
AOWWeq	88.288964	88.219519	88.037124	87.759386	87.345793	86.885413	86.333001	85.747354	85.332721	85.150919
BOCax	1.186098	1.186107	1.186108	1.186111	1.186120	1.186130	1.186147	1.186174	1.186184	1.186198

[a] *All bond lengths in Å, angles in °.*

Table S5. B3LYP Optimized variables of the dihedral angle scan, at the B3LYP level of theory

DSPIN	0	5	10	15	20	25	30	35	40	45
BWW	3.367564	3.365385	3.357152	3.344652	3.328927	3.311011	3.292854	3.276094	3.264940	3.260837
BCWeq	2.050460	2.050467	2.050414	2.050375	2.050355	2.050251	2.050192	2.050032	2.049957	2.049918
ACWWeq	87.074757	87.028042	86.908714	86.713119	86.440194	86.123182	85.741191	85.346919	85.049774	84.954740
BCWax	1.957723	1.957805	1.958353	1.959167	1.960220	1.961453	1.962736	1.964055	1.964969	1.965041
BOCeq	1.157383	1.157407	1.157481	1.157598	1.157731	1.157865	1.157978	1.158056	1.158072	1.158084
AOWWeq	87.920528	87.856168	87.688549	87.413078	87.026822	86.582565	86.045523	85.488928	85.069641	84.937037
BOCax	1.174288	1.174290	1.174274	1.174259	1.174244	1.174223	1.174221	1.174213	1.174208	1.174231

Table S6. Calculated CO, W-W and imaginary frequencies and IR intensities at the eclipsed D_{4h} geometry

				SCS-MP2		B3LYP		B3LYP 2Na	
	D_{4h} irrep	**Exp. ν / cm^{-1}**		**ν / cm^{-1}**	**IR intensity / km mol^{-1}**	**ν / cm^{-1}**	**IR intensity / km mol^{-1}**	**ν / cm^{-1}**	**IR intensity / km mol^{-1}**
CO	A_{1g}	2019	Raman	2012.38	0.00	2069.70	0.00	2075.77	0.00
CO	A_{2u}	1937	IR	1955.69	1085.36	1990.13	1085.36	2009.68	783.08
CO	B_{1g}	1960	Raman	1903.10	0.35	1966.19	0.35	1988.72	0.00
CO	E_u	1863	IR	1895.74	4368.02	1954.59	4368.02	1979.03	3894.70
CO	B_{1u}	-	-	1858.37	0.01	1928.79	0.01	1952.91	0.00
CO	E_g	1904	Raman	1827.38	0.00	1897.31	0.00	1924.56	0.00
CO	A_{1g}	1794	Raman	1812.19	0.00	1865.75	0.00	1808.16	0.00
CO	A_{2u}	1772	IR	1794.88	3258.81	1850.15	3258.81	1792.85	3055.36
W-W	A_{1g}	97	Raman	100.20	0.01	88.19	0.01	91.99	0.00
W-W twist	A_{2g}	-	-	26.60*i*	-	26.39*i*	-	25.63*i*	-
Na	A_{1g}, A_{2u}	-	-	-	-	-	-	65.03*i*, 69.41*i*	-

Table S7. Calculated CO, W-W and imaginary frequencies and IR intensities at the staggered D_{4d} geometry

				SCS-MP2		B3LYP		B3LYP 2Na	
	D_{4d} irrep	**Exp ν / cm^{-1}**		**ν / cm^{-1}**	**IR intensity / km mol^{-1}**	**ν / cm^{-1}**	**IR intensity / km mol^{-1}**	**ν / cm^{-1}**	**IR intensity / km mol^{-1}**
CO	A_1	2019	Raman	2011.99	0.07	2068.69	0.00	2077.97	0.00
CO	B_2	1937	IR	1951.85	727.93	1988.22	1110.72	2007.39	544.34
CO	E_1	1863	IR	1893.77	4313.89	1951.33	4068.49	1976.63	3871.40
CO	E_2	1960	Raman	1882.76	0.03	1947.39	0.00	1971.00	200.00
CO	E_3	1904	Raman	1827.56	0.01	1898.92	0.00	1926.34	0.01
CO	A_1	1794	Raman	1809.78	5.21	1864.71	0.01	1806.67	0.01
CO	B_2	1772	IR	1793.60	3692.31	1848.48	3083.97	1790.16	3706.87
W-W	A_1	97	Raman	117.49	0.01	105.37	0.00	106.47	0.00
Na	A_1,B_2							64.04*i*, 69.31*i*	

References

1. G. M. Sheldrick, *Acta Cryst. Sect. A*, 2015, **71**, 3.

2. CrysAlisPRO version 39.46, Oxford Diffraction /Agilent Technologies UK Ltd, Yarnton, England.

3. G. M. Sheldrick, *Acta Cryst. Sect. C*, 2015, **71**, 3.

4. O. V. Dolomanov, L. J. Bourhis, R. J. Gildea, J. A. K. Howard, H. Puschmann, *J. Appl. Cryst*., 2009, **42**, 339.

5. L. J. Farugia, *J. Appl. Cryst.*, 2012, **45**, 849.

6. Persistence of Vision (TM) Raytracer, Persistence of Vision Pty. Ltd., Williamstown, Victoria, Australia.

7. MOLPRO, version 2018.2, a package of ab initio programs, H.-J. Werner, P. J. Knowles, G. Knizia, F. R. Manby, M. Schütz, and others , see https://www.molpro.net.

8. A. D. Becke, *J. Chem.Phys*., 1993, **98**, 5648.

9. C. Lee, W. Yang, R. G. Parr, *Phys. Rev. B*, 1988, **37**, 785.

10. S. H. Vosko, L. Wilk, M. Nusair, *Can. J. Phys*., 1980, **58**, 1200.

11. J. P. Perdew, K. Burke, M. Ernzerhof, *Phys. Rev. Lett*., 1996, **77**, 3865.

12. S. Grimme, J. Antony, S. Ehrlich, H. Krieg, *J. Chem. Phys*., 2010, **132**, 154104.

13. I. Hyla-Kryspin and S. Grimme O*rganometallics,* 2004, **23**, 5581-5592.

14. T. Schwabe, Stefan Grimme, and Jean-Pierre Djukic *J. Am. Chem. Soc.*, 2009, **131,** 14156-14157.

15. S. Grimme, J. Antony, S. Ehrlich, H. Krieg, *J. Chem. Phys*., 2010, **132**, 154104.

16. F. R. Manby, P. J. Knowles, A. W. Lloyd, *J. Chem. Phys*., 2001, **115**, 9144.

17. H. -J. Werner, F. R. Manby, P. J. Knowles, *J. Chem. Phys*., 2003, **118**, 8149.

18. F. Weigend, R. Ahlrichs, Phys. Chem. *Chem. Phys*., 2005, **7**, 3297.

19. F. Weigend, Phys. *Chem. Chem. Phys*., 2006, **8***,* 1057.

20. D. Andrae, U. Haeussermann, M. Dolg, H. Stoll, H. Preuss, *Theor. Chim. Acta*, 1990, **77**, 123.

21. G. Knizia, J. E. M. N. Klein, *Angew. Chem. Int. Ed.*, 2015, **54***,* 5518.

22. AIMAll (Version 17.11.14), T. A. Keith, T. K. Gristmill Software, Overland Park KS, USA, 2019 (aim.tkgristmill.com).